Journal of The Electrochemical Society, **159** (3) J67-J71 (2012)
0013-4651/2012/159(3)/J67/5/$28.00 © The Electrochemical Society

$BaSnO_3$ Thick Film as a Carbon Dioxide Sensor

L. M. Cavanagh,[a] P. Smith,[b] and R. Binions[a,c,*,z]

[a]*Department of Chemistry, University College London, London WC1H 0AJ, United Kingdom*
[b]*McGowan Smith Consultancy Limited, Oxford, Oxon OX2 8JL, United Kingdom*
[c]*School of Engineering and Materials Science, Queen Mary, University of London, London E1 4NS, United Kingdom*

$BaSnO_3$ has been prepared as porous screen-printed thick films gas sensors. The sensor material was characterized by scanning electron microscopy and X-ray diffraction. The sensors gas response was investigated by exposure to varying concentrations of CO_2 gas in synthetic air and mixtures of CO and CO_2 all at a variety of different operating temperatures. Finally the gas response was examined to potential interferant gases including humidity. It was found that at an operating temperature of 500°C and to a 2000 ppm pulse of CO_2 the sensors gave a gas response of 3.10, higher than current literature values for metal oxide materials. It was also found that increasing relative humidity enhanced the gas response in contrast to other approaches.
 [DOI: 10.1149/2.050203jes]

Manuscript submitted October 7, 2011; revised manuscript received November 22, 2011. Published December 30, 2011. This was Paper 2067 presented at the Montreal, QC, Canada, Meeting of the Society, May 1–6, 2011.

There exists a clear demand for CO_2 concentration monitoring for applications such as the assessment of indoor air quality,[1] food storage[2] and early fire detection.[3]

Currently, most CO_2 sensing requirements are met using optical and electrochemical devices. Optically based devices are expensive and present integration problems,[1] while electrochemical sensors present complex fabrication processes and humidity interference.[4] Solid-state sensors based on metal-oxide semiconductors potentially provide an attractive alternative, since they offer potential for a low-cost, easily manufactured, small form factor solution.

Studies have focused on mixed oxide systems such as $BaTiO_3$-CuO and CuO-$BaSnO_3$.[5,6] The sensing mechanism appears due to gas interaction on a p-n heterojunction. However, the sensitivity of these devices to concentrations of interest for indoor air quality (300 ppm to 2000 ppm) is too low.

Other studies have reported promising metal oxide candidates such as La-doped SnO_2 and $BiTiO_3$, which display reliable CO_2 sensing properties.[7–10] However, the CO_2 sensitivity was found to be significantly reduced in the presence of humidity. $Nd_2O_2CO_3$ has also been reported as a strong candidate for a CO_2 sensor.[11] In this case it was noted that the response of the material was enhanced in the presence of humidity.

This study presents the case for thick films of $BaSnO_3$ as a highly promising material for the sensing CO_2 in the 0 to 2500 ppm range. CO_2 sensing characteristics are investigated over a range of operating temperatures and relative humidity's. It is found that the presence of humidity enhances the CO_2 gas response.

Experimental

Ceramic grade $BaSnO_3$ material was sourced from a commercial supplier [Cerac], and sieved through a 325 mesh (~45 μm aperture). The raw $BaSnO_3$ powder was then made into a screen-printable ink by mixing with a printing vehicle made from butyl carbitol–ethyl cellulose and in a ratio such as to give a 55% solids loading. Mixing of the powders and vehicle was done in a planetary ball mill (Speedymill) for 3 minutes using 5 mm ceramic mixing media.

The sensor inks were screen printed using a DEK printer (Model 1202) onto alumina tiles patterned with a gold inter-digitated electrode pattern (spacing ~ 65 μm) on one side and a serpentine platinum heater track on the underside. Bond pads for providing electrical contacts to the electrodes and heater track were gold. The $BaSnO_3$ inks were printed to a dry print thickness of ~60 μm, which required 8 print cycles; after each print cycle the film was dried under an infrared lamp for 10 min.

Contacts to the sensors were formed by spot welding using a McGregor parallel gap welder (Model DC601), 50 μm diameter platinum wire from pads on the sensors to terminals set in polyphenylene sulfide headers.

The devices were on-chip fired at 600°C for 1 hr and typically operated 500°C. The sensor heater was kept at a constant temperature by incorporating it into a constant-resistance Wheatstone bridge.[12] A fixed potential difference was applied across the sensor electrodes and the resultant current recorded to obtain the sensor resistance.

Gas-sensing experiments were performed on a locally constructed test rig.[13] Laboratory synthetic air functioned as the carrier gas, which was mixed with the target gas to give the required concentration and humidity levels.[14] The water pressure was altered by mixing the gas stream with air that had been passed through distilled water at room temperature.

The effects of various processing parameters on the raw powders of $BaSnO_3$ were examined to assess their impact on CO_2 sensitivity. Processing parameters investigated (i) calcination (700°C for 1 hr), (ii) sieving (38 μm aperture size), (iii) solids loading (55%–70%) and (iv) milling time (3–9 minutes). The effects of the investigated process parameters on CO_2 sensitivity were largely insignificant. In total 12 samples were prepared and tested. All tests conducted a minimum of three times in order to examine the reproducibility and repeatability of the sensors performance.

SEM images were acquired on a JEOL 6301F field emission instrument. X-ray diffraction patterns were measured on a Bruker Gadds D8 diffractometer using monochromated (CuKα1+2) radiation in the reflection mode.

Results and Discussion

Materials characterization.— The X-ray diffraction pattern of the prepared material used in the gas sensing experiments matched the database pattern (ICDD powder diffraction standard number 00-015-0780) for $BaSnO_3$ (Figure 1).

The scanning electron microscope (SEM) images of Figure 2a and 2b are typically representative of the top surfaces of the screen printed sensors after on-chip firing at 600°C for 1hr. From these SEM images, the porous structure of the layers and grains sizes of approximately 0.5 μm or less can be seen.

Gas response characterization.— The CO_2 response profiles of the $BaSnO_3$ were generated by exposing the films to CO_2 in the concentration range 0–2500 ppm (in 500 ppm steps) at 50% relative humidity The target gases were carried on a base flow of wet synthetic air (79% nitrogen, 21% oxygen), delivered at a constant flow rate of 1 $L.min^{-1}$. In this study the sensitivity, S, of the gas response is represented as the ratio of R_g (resistance when exposed to target gas)

* Electrochemical Society Active Member.
z E-mail: r.binions@qmul.ac.uk

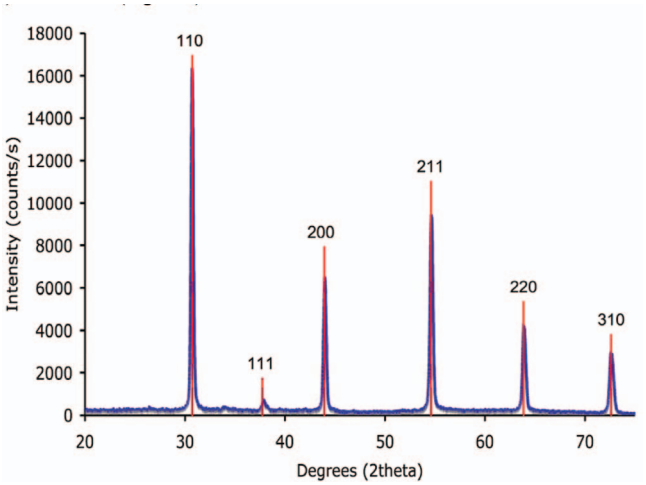

Figure 1. X-ray diffraction pattern for $BaSnO_3$ used in these experiments.

to R_0 (baseline resistance in the absence of target gas), as expressed in equation 1.

$$S = R_g/R_0 \quad [1]$$

In general, the higher the operating temperature the lower the CO_2 concentration at which saturation, (no further change in R_g as the gas concentration increased), tended to occur.

As expected the resistance of the $BaSnO_3$ films was highly dependent on operating temperature (Figure 3), with the resistance increasing sharply with decreasing temperature. At temperatures below about 300°C, it is reported/believed[17] that the Schottky barrier is too high to facilitate sufficient charge transfer across the grain boundaries, but between 400°C and 600°C the barrier height is greatly reduced while at the same time, the rate of reaction has increased significantly.[17]

Figure 4 shows the typical sensitivities exhibited by the $BaSnO_3$ thick film devices upon exposure to CO_2 for operating temperatures in the range 400°C to 500°C. In all cases a significant (reversible) resistance change is induced in the $BaSnO_3$ films upon exposure CO_2, with a maximum sensitivity (R_g/R_0) value of 3.15 (at 2500 ppm CO_2). Each sensor was able to discriminate between different CO_2 concentrations with the largest difference in response seen for a sensor operated at 500°C. It is likely at higher temperatures that thermal desorption becomes significant reducing the dynamic range of the sensor.

From Figures 5 and 6 it can be seen that for the range of temperatures tested, the overall sensitivity is maximized at an operating temperature of 500°C. However, although the sensitivity is maximized at 500°C, Figure 5 shows that better discrimination (wider dynamic range) between the similar CO_2 concentrations is achieved at the lower temperature of 400°C. Inspection of response plots (Figure 4) shows

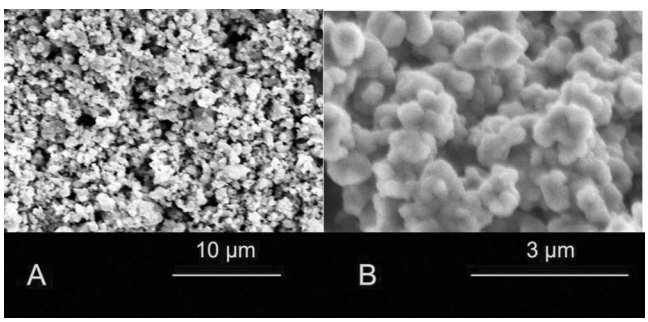

Figure 2. Typical SEM images of the $BaSnO_3$ sample surfaces after firing at 600°C.

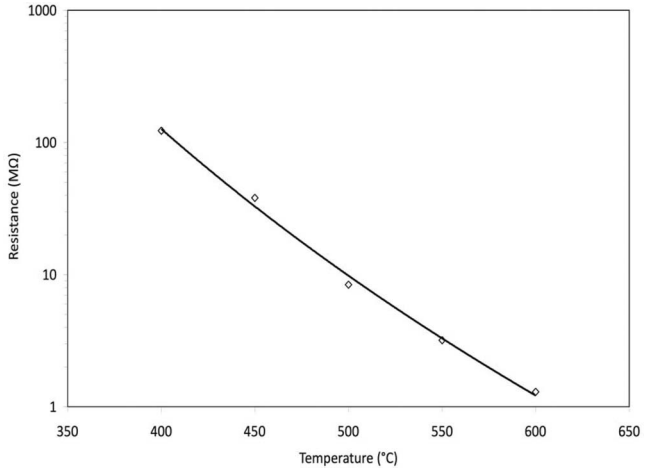

Figure 3. Dependence of baseline resistance on temperature in the range, 400–600°C, in synthetic air with 50% relative humidity.

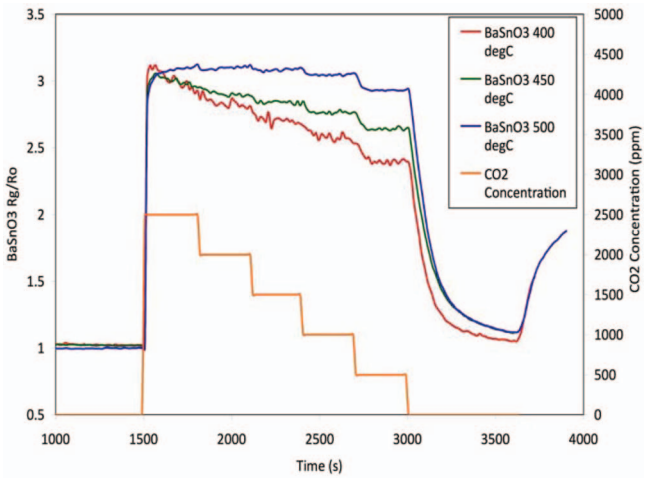

Figure 4. Response of $BaSnO_3$ sensors to varying concentrations of CO_2 gas in synthetic air with 50% relative humidity at different operating temperatures.

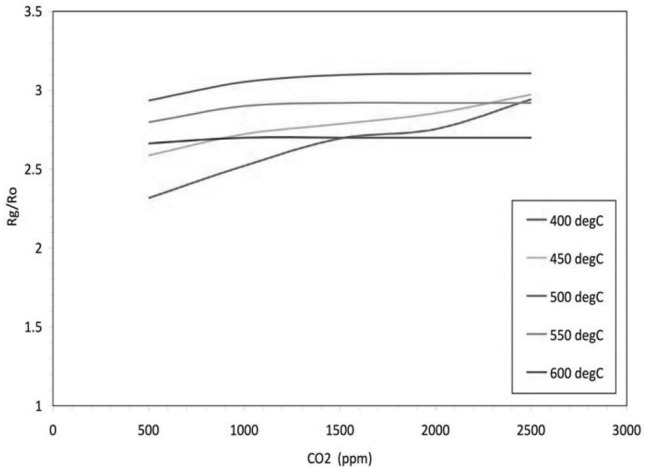

Figure 5. Response of $BaSnO_3$ sensors to varying concentrations of CO_2 gas in synthetic air with 50% relative humidity at different operating temperatures.

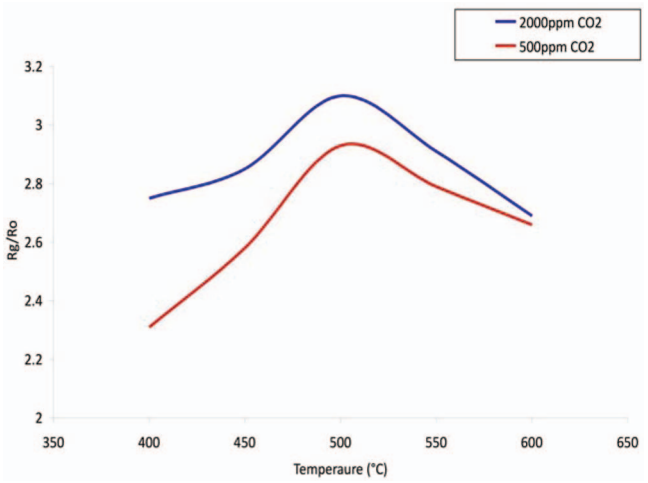

Figure 6. Response of $BaSnO_3$ sensors to fixed concentrations of CO_2 gas in synthetic air with 50% relative humidity at different operating temperatures.

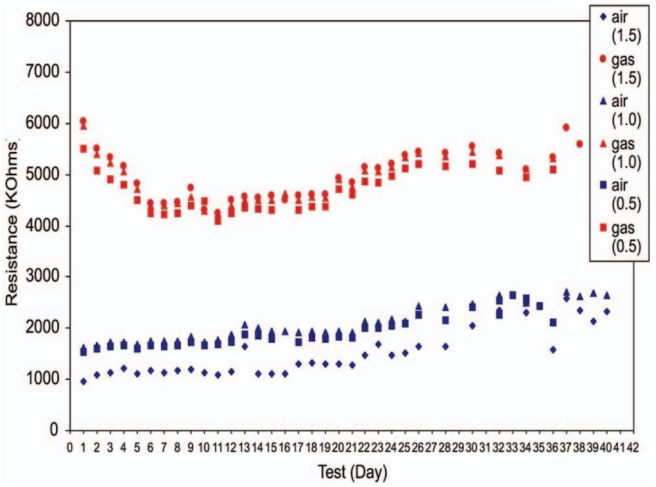

Figure 7. Gas sensor stability data of $BaSnO_3$ sensors operating at 500°C to varying flows of synthetic air and 5000 ppm CO_2 gas in synthetic air.

slowing recovery kinetics at 400°C and the feature of decreasing resistance with time, at the higher CO_2 concentrations. Figure 4 shows clearly that of a 2500 ppm concentration of CO_2, having the effect of an initial resistance increase becoming apparently less with time. This same effect is not observed for other reactive gases, and thus it is reasonable to conclude it can be associated directly with a surface reaction specific to CO_2.

Table I summarizes sensor responses and operating temperatures for a number of metal oxide based CO_2 sensors reported in the literature compared to our sensor. We report the highest sensor response with a comparable operating temperature to previously published work conducted with metal oxide sensor materials. Work has also been conducted with $Nd_2O_2CO_3$ (a metal oxide carbonate) that gives an impressive response of 7.5 to 3000 ppm CO_2 at an operating temperature of 350°C in 50% humidity air and a better dynamic range than our material.[11] However, the authors do not comment on the long-term stability of the material, it is well known that oxides of the lanthanide metals are the most thermodynamically stable.

Long term stability.— Figure 7 shows the longer-term stability data of the $BaSnO_3$ sensors. Tests were conducted at varying flows of gas and air for a 6-week period. It was found that after an initial 6 day period the baseline in gas and the baseline in air mirrored each other. As such after this initial 6 day period the sensors gave consistent responses as defined in equation 1.

Effects of interferant gases.— Figure 8 shows the effect of varying relative humidity on the $BaSnO_3$ baseline resistance and CO_2 response. The baseline resistance was seen to decrease with increasing relative humidity, from 14 MΩ at 30% relative humidity to 8 MΩ at 70% relative humidity. The figure also shows the response of the sensor to 1500 ppm and 500 ppm pulses of CO_2 in the presence of changing relative humidity levels.

Increasing from 70% relative humidity to 90% relative humidity had little further effect on either baseline resistance or the response magnitude (Figure 9). The effect of humidity on the baseline resistance of the $BaSnO_3$ film is in agreement with the general effect of humidity on semiconductor sensors as has been reported elsewhere.[18] In the case of SnO_2 it has been reported that increased conductivity with increased H_2O is due to the formation of hydroxyl on the film surface.[7]

Interestingly, the CO_2 sensitivity was enhanced with increasing humidity whereas in dry conditions (0% relative humidity, Figure 9) the CO_2 response was significantly diminished ($R_g/R_0 = 1.1$), to the point of being virtually non-existent. This behavior is in contrast to that reported for SnO_2, in which increasing relative humidity decreases CO_2 sensitivity.[7]

The response to CO was also investigated. Figure 10 shows the response of the sensors to CO, with and without the presence of CO_2. It is observed from that when both CO and CO_2 are present, the $BaSnO_3$ appears to respond to CO_2 only. Similarity in the two

Table I. Comparison of metal oxide sensor responses to 2000 ppm CO_2 in synthetic air as reported by Marsal et al.[3]

Material	Operating Temperature (°C)	Sensor Response (R_g/R_0)	Reference
SnO_2	100	1.1	15
SnO_2-La_2O_3	400	1.4	7
SnO_2-La_2O_3	400	1.6	10
SnO_2-LaOCl	425	1.4	3
$BaTIO_3$-CuO	500	1.6	16
$BaTIO_3$-CuO-La_2O_3	550	2.5	8
SnO_2-LaOCl	350	1.6	3 and 9
Our Material	500	3.1	

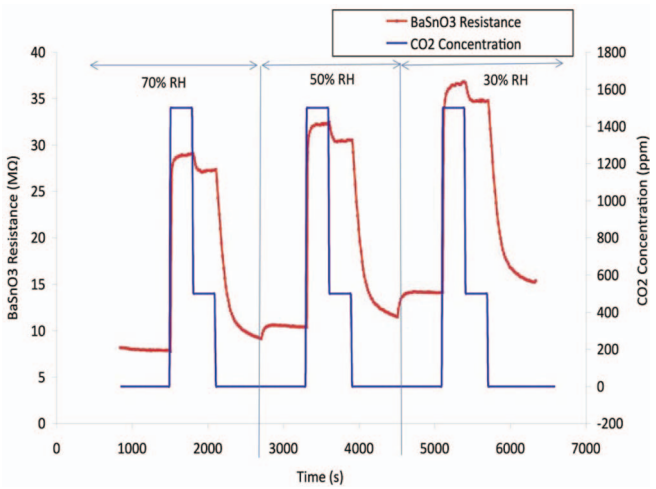

Figure 8. Effect of changing humidity levels on gas response of $BaSnO_3$ sensors operating at 500°C to varying concentrations of CO_2 gas in synthetic air.

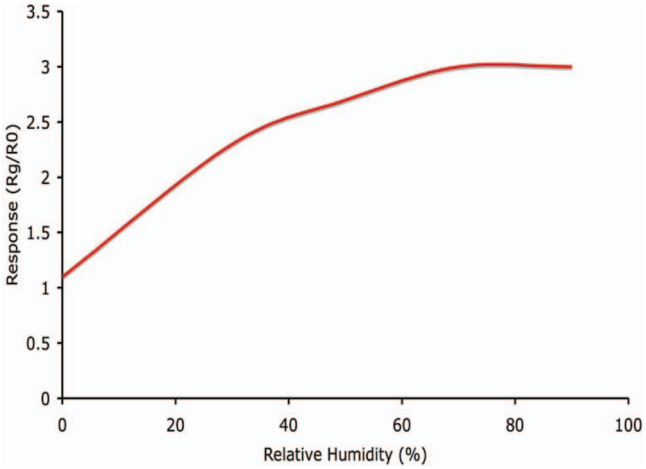

Figure 9. Plot of gas response vs relative humidity level for a $BaSnO_3$ sensor operating at 500°C to 2000 ppm of CO_2 gas in synthetic air.

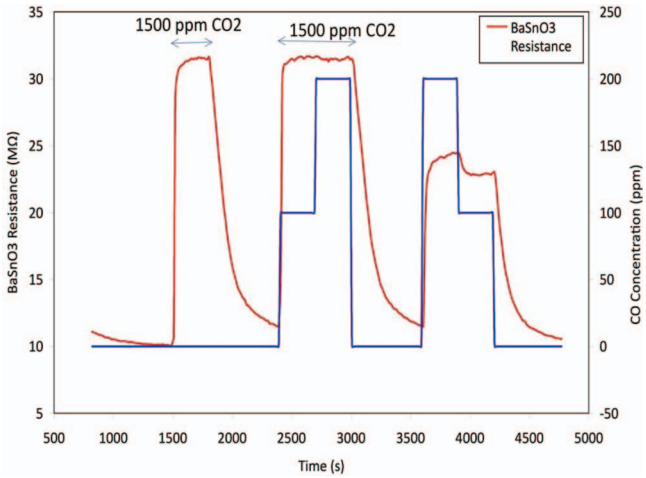

Figure 10. Response of $BaSnO_3$ sensors operating at 500°C to a constant concentration of CO_2 gas and varying concentrations of CO gas in synthetic air with 50% relative humidity.

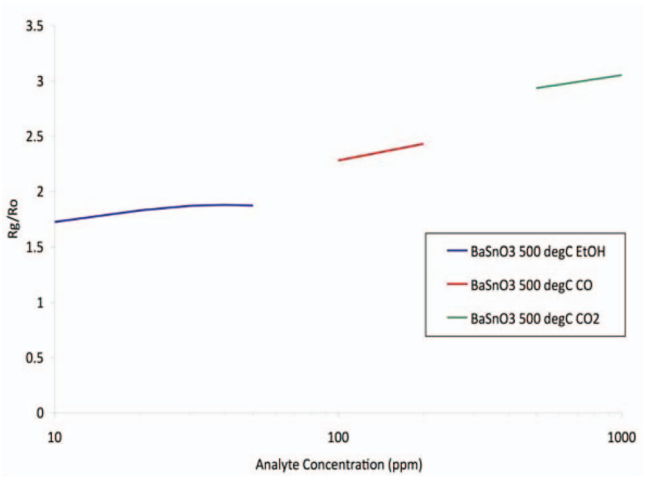

Figure 11. Response of $BaSnO_3$ sensors operating at 500°C to a variety of analytes at varying concentrations in synthetic air with 50% relative humidity.

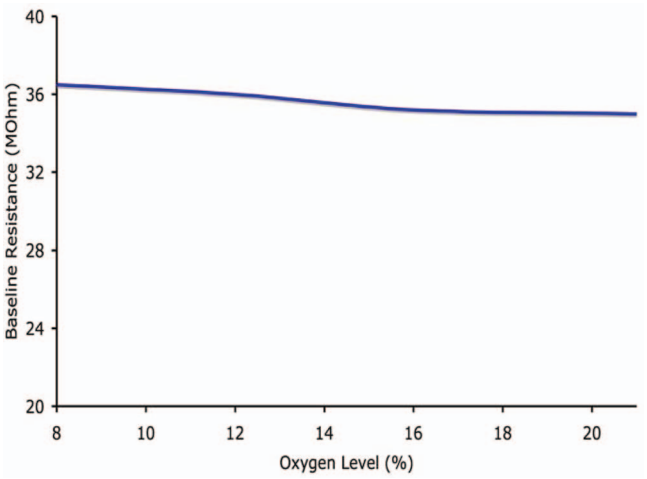

Figure 12. Plot of baseline resistance versus oxygen % for a $BaSnO_3$ sensor operated at 500°C.

responses response profiles suggest that the sensor response observed in the presence of CO could be due to CO_2 the resulting product from the oxidation of carbon monoxide.[9]

Figure 11 summarizes the sensitivities for the various analytes across a range of concentrations. The effect of varying levels of oxygen partial pressure was also examined (Figure 12). Oxygen concentration levels were reduced from 21% to 8% and it was observed that the resistances of the $BaSnO_3$ remained largely unchanged. This desirable characteristic is in contrast to that generally observed for pure SnO_2 films.[7]

The increase in resistance upon exposure to the reducing CO (Figure 10) and EtOH gases would appear to suggest that the $BaSnO_3$ is displaying p-type semiconductor behavior, when compared to the response of n-type SnO_2 to these gases.[3]

In attempting to propose a mechanism for the CO_2 sensing characteristics of $BaSnO_3$ thick film sensor, we begin by making reference to previous studies which indicate the formation of carbonates in barium[1,3] and lanthanum containing compounds.[3] More importantly, the formation of these carbonates has been observed to be rapidly reversible in the absence of CO_2.[3] It has also been shown that this reversible carbonate formation finds more favorable conditions in humid environments.[9,11] Considering these findings on reversible carbonate formation and the influence humidity in enhancing our CO_2 sensitivity, a reversible reaction such as that shown in equation 2 has been proposed as being a dominant factor in the sensing chemistry.[1]

$$BaCO_3 + H_2O + CO_2 \leftrightarrow Ba(HCO_3)_2 \qquad [2]$$

In a previous study, the presence of superficial carbonates, with the assistance of water, has been demonstrated to be of great importance in describing the interaction between CO_2 and the sensing film.[1,19] Previous work has demonstrated that the concentration of surface, hydroxyl and / or carbonates is important in determining the electrical properties of the material.[11] However, further work is required to establish the proposed effects of humidity-assisted reversible carbonate and / or hydrogen carbonate formation and clarify its role in the sensing mechanism.

Conclusions

$BaSnO_3$ prepared as porous screen-printed thick films and running at elevated temperature have been found to exhibit a significant resistance change upon exposure to CO_2 concentrations in the indoor air quality application range. The achieved CO_2 sensitivity of 3.10 at 2000 ppm (and 3.15 at 2500 ppm) is larger than the current highest reported literature values for other metal oxide systems. Film conductance changes upon interaction with CO_2 are most likely achieved via

the rapid and reversible formation of carbonates resulting in fast response and recovery times. Unlike certain other metal oxide sensors, the CO_2 sensitivity is enhanced with the presence of humidity. The dynamic range of the sensors is not as wide as desired; as such they are more suited to an alarm mode of application rather than continual monitoring.

Acknowledgments

RB thanks the Royal Society for a Dorothy Hodgkin fellowship and the EPSRC for financial support (grant number EP/H005803/1).

References

1. J. Herran, G. G Mandayo, and E. Castano, *Thin Solid Films*, **517**, 6192 (2009).
2. G. G. Mandayo, F. Gonz · lez, I. Rivas, I. Ayerdi, and J. Herran, *Sens. Act. B*, **118**, 305 (2006).
3. A. Marsal, A. Cornet, and J. R. Morante, *Sens. Act. B*, **94**, 324 (2003).
4. T. Ishihara, K. Kometani, Y. Mizuhara, and Y. Takita, *Sens. Act. B*, **13**, 470 (1993).
5. T. Ishihara, K. Kometani, Y. Mizuhara, and Y. Takita, *J. Electrochem. Soc.*, **139**, 2881 (1992).
6. T. Ishihara, K. Kometani, M. Hashida, and Y. Takita, *J. Electrochem. Soc.*, **138**, 173 (1991).
7. A. Marsal, G. Dezanneau, A. Cornet, and J. R. Morante, *Sens. Act. B*, **95**, 266 (2003).
8. D. H. Kim, J. Y. Yoon, H. C. Park, and K. H. Kim, *Sens. Act. B*, **62**, 61 (2000).
9. N. Mizuno, T. Yoshioka, K. Kato, and M. Iwamoto, *Sens. Act. B*, **13**, 473 (1993).
10. M.-S. Lee and J.-U. Meyer, *Sens. Act. B*, **68**, 293 (2000).
11. I. Djerdj, A. Haensch, D. Koziej, S. Pokhrel, N. Barsan, U. Weimar, and M. Niederberger, *Chem. Mater.*, **21**, 5375 (2009).
12. R. Binions, H. Davies, A. Afonja, S. Dungey, D. Lewis, D. E. Williams, and I. P. Parkin, *J. Electrochem. Soc.*, **156**, J46 (2009).
13. S. C. Naisbitt, K. F. E. Pratt, D. E. Williams, and I. P. Parkin, *Sens. Act. B*, **114**, 969 (2006).
14. G. S. Henshaw, D. H. Dawson, and D. E. Williams, *J. Mater. Chem.*, **5**, 1791 (1995).
15. J. Cerda, J. Arbiol, G. Dezanneau, R. DÌaz, and J. R. Morante, *Sens. Act. B*, **84**, 21 (2002).
16. J. Tamaki, M. Akiyama, C. Xu, N. Miura, and N. Yamazoe, *Chem. Lett.*, **19**, 1243 (1990).
17. T. Ishihara, K. Kometani, Y. Mizuhara, and Y. Takita, *Sens. Act. B*, **5**, 97 (1991).
18. G. Ghiotti, A. Chiorino, G. Martinelli, and M. C. Carotta, *Sens. Act. B*, **25**, 520 (1995).
19. A. Prim, E. Pellicer, E. Rossinyol, F. Peiró, A. Cornet, and J. R. Morante, *Adv. Funct. Mater.*, **17**, 2957 (2007).